Cell Tissue Res (1992) 267:437–448

Cell & Tissue Research

Morphology and function of capillary networks in subregions of the rat tuber cinereum*

Steven W. Shaver, Judy J. Pang, Dan S. Wainman, Katharine M. Wall, and Paul M. Gross

Neurosurgical Research Unit, Departments of Surgery and Physiology, Queen's University and Kingston General Hospital, Kingston, Ontario, Canada K7L 3N6

Received February 25, 1991 / Accepted November 13, 1991

Summary. The differentiated cytology, cytochemistry, and functions within subdivisions of the tuber cinereum prompted this morphometric and physiological investigation of capillaries in the median eminence and arcuate nucleus of albino rats. Morphometric studies established that the external zone of the median eminence had 3–5 times the number and surface area of true and sinusoidal capillaries than the internal or subependymal median eminence zones, or either of two subdivisions examined in the arcuate nucleus. Type-I true capillaries, around which Virchow-Robin spaces comprise 1% of arcuate tissue area, were situated proximally to the median eminence border. This finding is consistent with a premise that confluent pericapillary spaces enable infiltration of arcuate neurons by factors from capillary blood from the median eminence or Virchow-Robin spaces. Physiologically, the rate of penetration across the median eminence capillaries by blood-borne [^{14}C]α-aminoisobutyric acid (a neutral amino acid used as a capillary permeability tracer) was 142 times greater than for capillaries in the distal arcuate nucleus within 12 s of tracer administration. A new finding was that the proximal arcuate nucleus had a permeability × surface area product of 69 μl g^{-1} min^{-1}, 34 times greater than that in more distal aspects of the tuber where blood-brain barrier properties exist. We also found that the microcirculatory transit time of a plasma space marker, [^{14}C]sucrose, was considerably longer (1.2 s) in the median eminence and proximal arcuate nucleus than in the distal arcuate or ventromedial nucleus (0.4 s). By virtue of its high capillary permeability and extensive blood-tissue surface area, including the wide Virchow-Robin spaces, the median eminence external zone could be a gateway for flooding other tuberal compartments with blood-borne factors. This effect may be compounded by capillary bed specializations in the proximal arcuate nucleus where Type-I true capillaries, Type-III sinusoids, and pericapillary spaces are confluent with those in the median eminence. The results indicate that the proximal arcuate parenchyma could be exposed to circulating neuroactive substances on a moment-to-moment basis.

Key words: Median eminence – Arcuate nucleus – Endothelial cells – Capillary permeability – Blood flow – Quantitative autoradiography – Rat (Sprague-Dawley)

The mediobasal hypothalamus (tuber cinereum), median eminence, and pituitary gland are major sites of integrated endocrine regulation by the central nervous system. Although primary control of the tuberoinfundibular system by hypothalamic nuclei is an accepted concept (e.g., Palkovits 1982), there is considerable anatomical evidence for bidirectional communication between distinct tuberal structures, i.e., for the modification of hypothalamic activity by neuroactive substances originating as adeno- or neurohypophysial secretions or from systemic blood irrigating the permeable capillaries of the median eminence.

Potential avenues of contact between subregions of the tuber and pituitary gland are multifarious, and include (1) neural fibers passing through the median eminence internal zone or terminating on capillaries of the primary portal plexus in the external zone (reviewed by Mezey and Palkovits 1982), (2) two-way ependymal transport of messenger substances along tanycytic processes (reviewed by Rodríguez 1976), (3) retrograde axoplasmic transport, as demonstrated with horseradish peroxidase (HRP), from cell processes neighboring neurohypophysial blood vessels to hypothalamic perikarya (Broadwell and Brightman 1976, 1983), (4) retrograde blood flow from the pituitary gland via the infundibular stalk to the median eminence and hypothalamus (reviewed by Szentágothai et al. 1968; Page 1982), (5) anastomoses of median eminence capillaries extending to

* Dedicated to Dr. Milton W. Brightman of Bethesda, Maryland, USA on the occasion of his 67th birthday and tribute as Craigie Scholar at the First Craigie Conference on Brain Capillaries, Toronto, Ontario, June 24, 1990

Offprint requests to: P.M. Gross

proximal regions of the adjacent arcuate nucleus (reviewed by Duvernoy 1972; Ambach et al. 1976; Page et al. 1978), and (6) pericapillary (Virchow-Robin) spaces in confluence between microvessels of the median eminence external zone and those in other median eminence zones and the proximal arcuate nucleus (Leonhardt and Eberhardt 1972; Krisch et al. 1978; Krisch and Leonhardt 1989). The first four avenues have been demonstrated convincingly (see above references). The latter two, concerning the subregional distribution and function of capillaries and Virchow-Robin spaces, are less appreciated with respect to their potential significance as functional pathways contributing to a moderation of tuberal activities.

Previous investigators have reported qualitative studies in which circulating markers, such as HRP, labeled proteins, or sodium fluorescein, present in systemic blood for periods of minutes to hours, not only invaded the median eminence pervasively but also breached proximal portions of the hypothalamic arcuate nucleus wherein blood-brain barrier (BBB) properties were thought to reside (Wsniewski and Olszewski 1963; Brightman et al. 1975; Broadwell and Brightman 1976; Krisch et al. 1978; van den Pol and Cassidy 1982; Balin et al. 1986; Martinez and Koda 1988). As previously suggested (Leonhardt and Eberhardt 1972; Krisch et al. 1978), confluent pericapillary spaces probably provide an important transport pathway for such dispersal of neurohumoral factors from the median eminence into tuberal territories. This concept is important because it implies that the regulation of amine- and peptide-synthesizing neurons in the arcuate nucleus, such as those for dopamine (Hökfelt and Fuxe 1972) and pro-opiomelanocortin (Kiss et al. 1985), could be under some degree of control by substances originating from systemic blood or axon terminals penetrating Virchow-Robin spaces of the capillaries of the median eminence (Krisch et al. 1978; van den Pol and Cassidy 1982). The time constant over which this process occurs, however, has never been estimated.

Since an improved understanding of blood-brain solute exchange is thus necessary to further delineate neuroendocrine mechanisms in the tuber cinereum, we conducted a comprehensive morphometric and physiological analysis of capillaries in subregions of the median eminence and arcuate nucleus. We specifically tested the hypothesis that the tuberal-arcuate interface region, which exhibits microvascular anastomoses and shared pericapillary spaces, would display physiological characteristics resembling more those of the median eminence than those of hypothalamic nuclei distant from the infundibulum, such as the ventromedial nucleus wherein BBB characteristics exist (Gross et al. 1986). We further examined whether the *rate and amount* of penetration into the proximal arcuate nucleus by a blood-borne marker would be similar to those in the median eminence.

Materials and methods

Topography and morphometry

Five male Sprague-Dawley rats (325–425 g) were anesthetized with sodium pentobarbital and perfused transcardially through a cannula in the left ventricle with heparinized 0.1 M phosphate buffer, pH 7.4, at 37° C and 40–60 mm Hg. The animals were then perfused with 2% paraformaldehyde, 2% glutaraldehyde, 4% sucrose, and 0.05% calcium chloride in 0.1 M phosphate buffer. The brains were removed and stored in fixative overnight.

We used a Vibratome to cut 400-μm-thick coronal sections through the entire longitudinal extent of the median eminence from which we further marked and dissected the tissue for isolation of portions of the median eminence and arcuate nucleus where the latter structure borders laterally with the ventromedial nucleus (e.g., see Paxinos and Watson 1986; Figs. 28–31); this level is also notable by its clear topographical differentiation of immunoreactivity for pro-opiomelanocortin (POMC) perikarya and fiber terminals (see Figs. 1–4 of Mezey et al. 1985). Thus, our sections lay between 2300 and 3300 μm caudal from bregma.

Subsequently, the sections were rinsed several times with buffer, postfixed in buffered 1% osmium tetroxide, and stained en-bloc with aqueous 4% uranyl acetate for 1 h. The sections were further dehydrated through a graded series of alcohols, infiltrated with propylene oxide, then embedded in Epon 812. From each tissue block, we cut sections of 1 μm thickness using glass knives, stained them with 1% toluidine blue, and cataloged them according to orientation. Photographs of the sections were taken with a Leitz Vario-Orthomat at 30× magnification and enlarged a further 8× during printing for a final print magnification of 240×. In some cases, we enlarged specimens further (by 4×) during analysis by application of a zoom function in the imaging system software (below).

Capillaries were identified as the smallest microvessel profiles devoid of smooth muscle and were analyzed using a micro-computer imaging device (MCID; Imaging Research Inc., St. Catharines, Ontario, Canada) according to stereological theory and equations used previously (Weibel et al. 1966; Sposito and Gross 1987a, b). Vessels were categorized as 'true' capillaries, luminal diameter of 3–7.5 μm, or 'sinusoidal' capillaries, 7.5–20 μm diameter (Rhodin 1974). Measurements included the number, area, perimeter, and average diameter of capillaries, and the total tissue area analyzed. MCID then computed capillary density (number of capillaries per mm^2 of tissue), volume fraction (% volume of capillaries in the tissue area), and surface area ($S_v = \pi\, dL \times 10^{-3}$, where L is the length per unit volume of capillaries and d is the average capillary diameter). MCID also allowed assessment of the pericapillary space fraction (total area of pericapillary space/total tissue area).

We obtained data from five enlarged photomicrographs of the median eminence and arcuate nucleus from each of five rats. Three zones of the median eminence (subependymal zone, internal zone, and external zone see Fig. 1) and two subdivisions of the arcuate nucleus (one proximal to and the other distal from the median eminence) were examined. We then analyzed the results using single-factor analyses of variance in a repeated-measures design and Tukey multiple comparison tests. Thus, capillary density, volume fraction, surface area, diameter, and pericapillary space fraction were compared across the median eminence and arcuate nucleus zones.

For electron-microscopic studies of capillaries, we obtained (from the same Epon blocks) ultrathin, pale-gold sections, ~70 nm in thickness. These were placed on 150-Hex grids and stained with uranyl acetate and lead citrate. To facilitate examination under the electron microscope, the sections were divided into median eminence and hypothalamic subdivisions, then photographed at magnifications of 5000 to 10000× using an Hitachi H-7000 transmission electron microscope. From material for each rat, at least five prints were examined for the five subregions described.

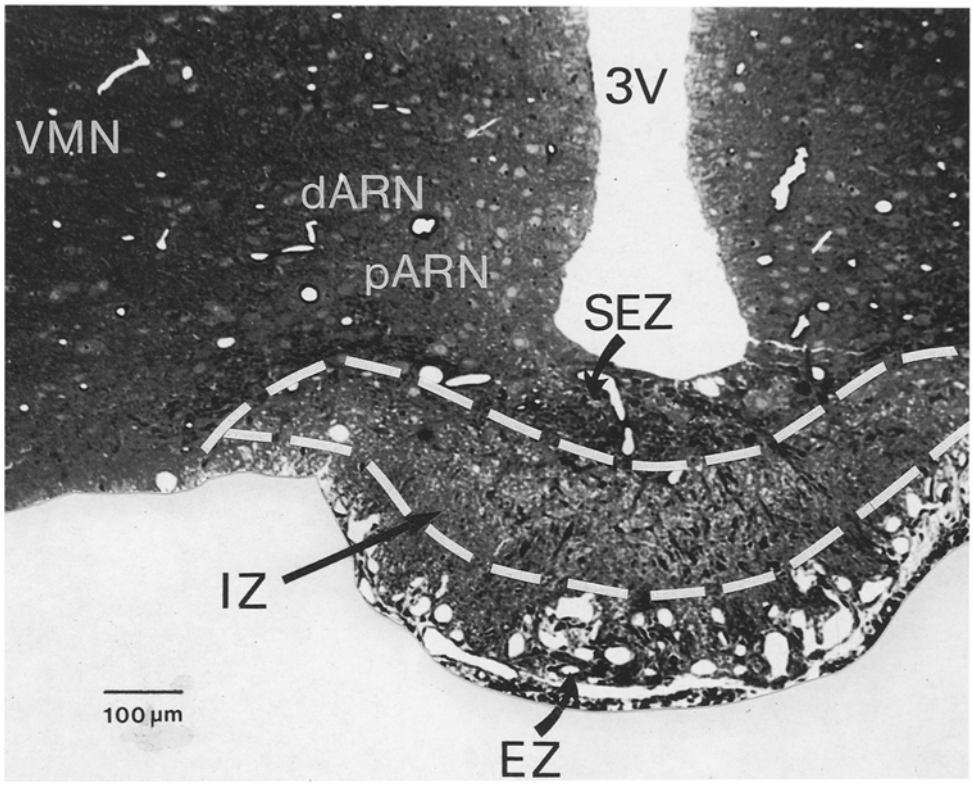

Fig. 1. Stained 1-µm-thick section (toluidine blue) of the median eminence and arcuate nucleus showing the three zones in the median eminence and the two subregions of the arcuate nucleus analyzed. This section is at a similar magnification to those used for morphometric analyses of capillaries with the imaging system, which permitted further magnification as needed. *3V* 3rd ventricle; *SEZ* subependymal and ependymal zone of the median eminence; *IZ* internal zone of the median eminence; *EZ* external zone of the median eminence; *pARN* proximal arcuate nucleus; *dARN* distal arcuate nucleus; *VMN* ventromedial nucleus. ×178

Microvasular physiology

All physiological measurements were obtained from conscious, lightly-restrained rats, as described previously (Gross et al. 1987). Briefly, the rats were anesthetized in a box with a mixture of 3% halothane in nitrous oxide and oxygen, and were maintained in this state during surgical operations by breathing the gas mixture through a nose cone. Into both femoral arteries and one femoral vein, we inserted polyethylene catheters that were allowed to protrude from a loose-fitting plaster cast over the pelvis and hindquarters. When dry, the cast was taped to a lead block, and the rats were allowed 2–3 h (body temperature being maintained under a heat lamp) to recover from the anesthesia before assessment of physiological status. We determined arterial blood pressure and blood gases, plasma ion and glucose concentrations, hematocrit, and rectal temperature.

Comprehensive quantitative measurements of capillary permeability entailed the derivation of permeability × surface area (PS) products (e.g., Blasberg et al. 1983a; Gross et al. 1987), which required separate determinations or estimates of (1) the distribution (exchangeable) volume for a plasma space marker, (2) the capillary blood flow, and (3) the rate of unidirectional transfer from blood to tissue for a circulating tracer.

Microvascular exchangeable volume (Ohno et al. 1978; Gross et al. 1990), V_e, was assessed using [^{14}C]sucrose (MW = 342 Da, 125 µCi kg^{-1}) given to 6 conscious rats. Following iv injection, the tracer was allowed to circulate for 30 s (see Gross et al. 1990, for critical discussion of this circulation time) and arterial blood was sampled several times to evaluate plasma ^{14}C concentration. Rats were killed by rapid iv injection of sodium pentobarbital followed by concentrated KCl.

Capillary blood flow, F, was determined with iodo[^{14}C]antipyrine (125 µCi kg^{-1}; Sakurada et al. 1978) infused in experiments of 25-s duration in 5 conscious rats. The tracer was given by ramp infusion iv (Gross et al. 1987, 1990), multiple arterial blood samples of about 70 µl volume were taken over the course of the experiment, and the rats killed by decapitation.

Blood-to-tissue transfer, K, of the neutral amino acid, [^{14}C]α-aminoisobutyric acid (AIB, MW = 103 Da), was derived after iv injection and 12-s circulation times in 6 conscious rats (Blasberg et al. 1983a, b; Gross et al. 1986, 1987, 1990). We sampled arterial blood continuously into separate vials throughout the study and killed the rats by decapitation. These experiments of 12-s duration were employed to estimate unidirectional transfer during only one high-concentration pass of the tracer through the microcirculation. Transfer was assumed to be unidirectional over the course of the experiment following the theory and application of the AIB method for assessment of capillary permeability in brain (Blasberg et al. 1983a, b).

Tissue preparation for autoradiographic analysis

At the conclusion of each physiological experiment, brains were removed rapidly and frozen in 2-methylbutane cooled in dry ice to −45° C. Serial sections (20 µm thick) throughout the median eminence region, 2000–3000 µm caudal from bregma, were taken onto glass coverslips in a microtome cryostat at −17° C, then dried on a slide tray at 65° C. Every fourth section was collected on glass slides for histological staining with thionin heated to 60° C.

Sections for autoradiography were glued to cardboard, numbered in order, and placed in cassettes for 2–4 weeks with Kodak OM-1 film and [^{14}C]methylmethacrylate standards calibrated for their equivalence to levels of ^{14}C radioactivity assessed in 20-µm-thick sections of rat brain.

Quantitative densitometric analysis of the autoradiographs was performed with the MCID system, which permitted determinations of tissue ^{14}C concentrations by referencing tissue optical densities to those of the standards. Readings were obtained from a minimum of 6 sections per animal. The resulting tissue and plasma ^{14}C con-

centrations, and experimental times for each of the above techniques, were used to calculate the values described below.

The MCID software was used to digitally overlay the autoradiograph with an image of adjacent histology. Each was digitized and magnified (10–30×) on the screen, and then they were brought into alignment by adjusting the position of the specimen on the stage. We obtained densitometric readings using sample windows positioned precisely within histologically defined subregions. This procedure allowed us to gather autoradiographic data while viewing the histology, thus increasing the precision of the subregional analyses.

Calculations

Microvascular exchangeable volume, $V_e = A_m/C_p$, (Eq. 1) was expressed in units of μl g^{-1}, where A_m is the amount of radioactivity in 1 g of brain and C_p is the radioactivity concentration in 1 ml of arterial plasma (Ohno et al. 1978; Blasberg et al. 1983a, b; Gross et al. 1987).

Capillary blood flow,

$$F = \frac{A_m}{\int_0^T C_p(t) \exp[-k_0(T-t)]\, dt}$$

(Eq. 2) was expressed in units of μl g^{-1} min^{-1},

where A_m and C_p are defined as above, k_0 represents the relationship between the rate of blood flow per g of tissue and the blood/tissue partition coefficient for iodoantipyrine (0.8), and T and t are the experimental times (Sakurada et al. 1978; Gross et al. 1987, 1990).

Blood-brain influx of [^{14}C]AIB,

$$K = \frac{A_m - (V_e \times C_T)}{\int_0^T C_p(t)\, dt},$$

(Eq. 3) was expressed in units of μl g^{-1} min^{-1},

where C_T is the terminal plasma ^{14}C concentration and the other variables are as defined above. The product of $V_e \times C_T$ is a correction term of small value to estimate the amount of tracer remaining in capillary plasma at the conclusion of the experiment (Ohno et al. 1978; Blasberg et al. 1983a, b; Gross et al. 1987, 1990).

For calculating rates of plasma flow from the values for whole blood flow, the median eminence was assigned a tissue hematocrit of 28%, whereas the arcuate and ventromedial nuclei were regarded as gray matter regions with tissue hematocrits of 32% (see Table 1 of Gross et al. 1987). Values of tissue hematocrit (*THct*) were applied to derive rates of capillary plasma flow (F_p) from individual values of F,

$F_p = F \times (1 - THct)$ (units of μl g^{-1} min^{-1}, Eq. 4)

In addition, an extraction fraction (E) was calculated for AIB,

$E = (K/F_p) \times 100$ (units of %, Eq. 5)

and permeability × surface area (*PS*) products by

$PS = -F_p \times \ln(1 - E)$ (units of μl g^{-1} min^{-1}, Eq. 6)

(see Renkin 1959; Crone 1963; Blasberg et al. 1983a, b; Gross et al. 1986, 1987, 1990).

Finally, the transit time (tt) for the tracer sucrose through individual microvascular beds was estimated from

$tt = V_e/F_p$ (units of *s*, Eq. 7)

(see Gross et al. 1986, 1987, 1990).

Table 1. Summary of tuberal capillary types. "True" capillaries were defined in the present study as those vessels with luminal diameters between 3 and 7.5 μm (means of 4.5–5.3 μm, data in Table 2). "Sinusoids" were defined as capillary-like vessels having luminal diameters >7.5 μm (means of 10.8–12.3 μm, data in Table 2). Type-I capillaries were found in the internal and subependymal zones of the median eminence, and in the proximal arcuate nucleus. Type-II capillaries were identified in both zones of the arcuate nucleus. Type-III capillaries were present in the internal and external zones of the median eminence. Sinusoids were located in all zones of the median eminence and in the proximal arcuate nucleus (Table 2). For references, see Marchesi and Barrnett (1964), Rhodin (1974), Shaver et al. (1990, 1991) and Gross (1991)

	Density of vesicles	Density of fenestrations	Pericapillary spaces	Presumed rate of transcapillary solute transfer
True capillaries				
I	moderate	absent	perceptible	moderate
II	low	absent	absent	low
III	high	high	large	high
Sinusoids	high	high	large	high

Statistical analysis

Data from the MCID system were analyzed using a separate statistics program (SAS; SAS Institute Inc., Cary, N.C., USA). Data for one variable across the subregions were evaluated by a single-factor analysis of variance at the 0.05 level of significance. Where significant F ratios resulted, we tested the data further by using the Tukey method to calculate critical differences between group means.

Results

Topography and morphometry

Definition of capillary types and tuberal zones. We followed previous morphological definitions of capillaries in three categories (Types I, II, and III) based on their fine structure and extent of pericapillary spaces (Table 1).

Three dorsoventral zones of the median eminence were delineated (Fig. 1). The subependymal zone was identified histologically as the part of the median eminence bordering the third ventricle, with an average ependymal layer depth of 100 μm from the infundibular recess and a tissue area of 0.02 mm^2 per section. The most ventral portion of the median eminence, characterized by a rich density of sinusoids and Type-III capillaries (Fig. 2A) with extensive pericapillary spaces in the portal plexus, was termed the external zone; it measured approximately 100 μm in depth and 0.05 mm^2 in the analyzed area per section. The remainder of the median eminence, which lay between the subependymal and external zones, and which thus included the palisade zone dorsal to the portal plexus (Rodríguez 1972) and fibers en passant, was analyzed as the internal zone; it measured about 150 μm in dorsoventral thickness and 0.05 mm^2 in area per section. Capillaries both of Type I and III morphology were found in this zone (e.g., Fig. 2A, B).

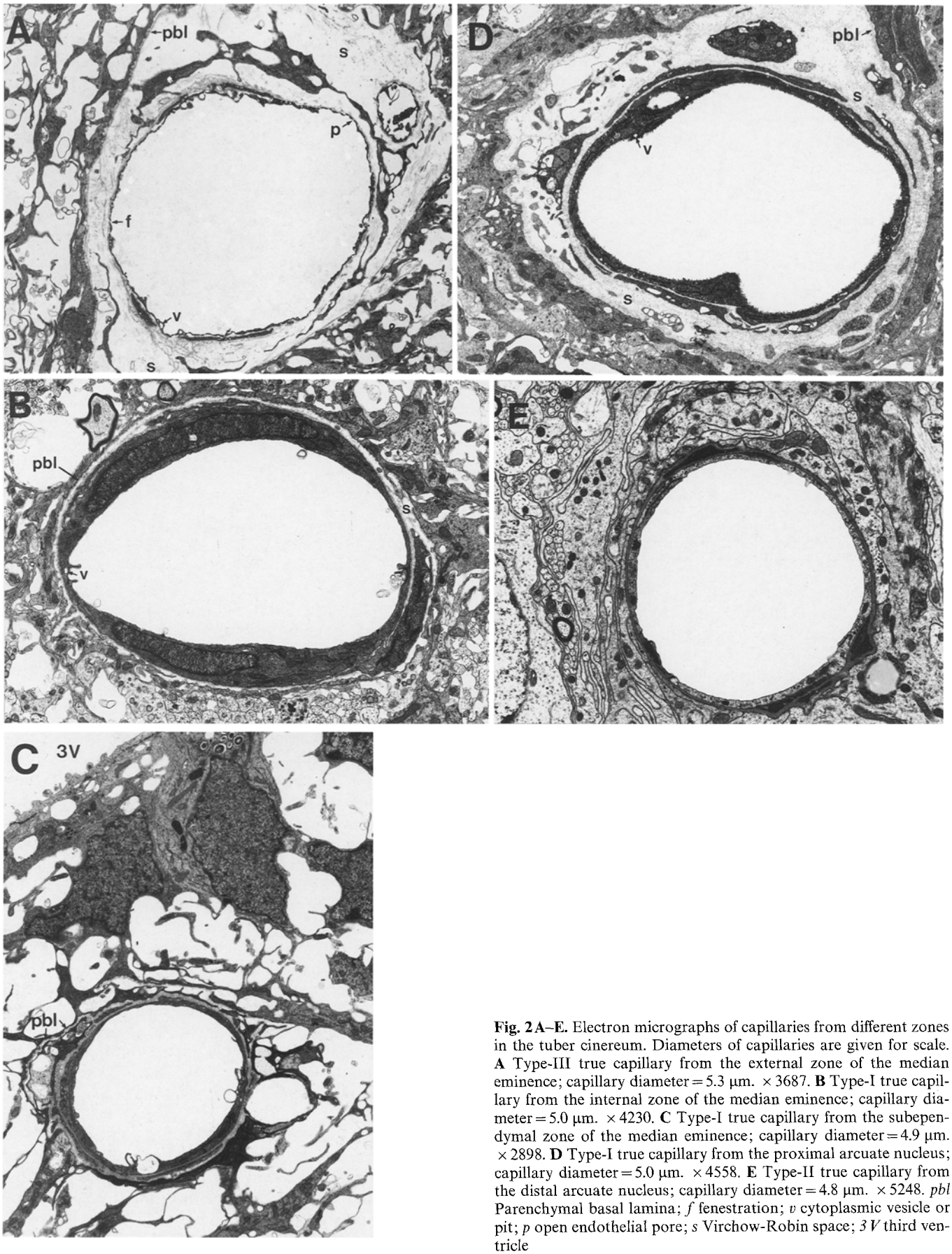

Fig. 2A–E. Electron micrographs of capillaries from different zones in the tuber cinereum. Diameters of capillaries are given for scale. **A** Type-III true capillary from the external zone of the median eminence; capillary diameter = 5.3 μm. × 3687. **B** Type-I true capillary from the internal zone of the median eminence; capillary diameter = 5.0 μm. × 4230. **C** Type-I true capillary from the subependymal zone of the median eminence; capillary diameter = 4.9 μm. × 2898. **D** Type-I true capillary from the proximal arcuate nucleus; capillary diameter = 5.0 μm. × 4558. **E** Type-II true capillary from the distal arcuate nucleus; capillary diameter = 4.8 μm. × 5248. *pbl* Parenchymal basal lamina; *f* fenestration; *v* cytoplasmic vesicle or pit; *p* open endothelial pore; *s* Virchow-Robin space; *3V* third ventricle

Table 2. Morphometry of capillaries in median eminence and arcuate nucleus zones

	Total area of tissue sampled (mm^2)	Total no. of capillaries measured	Density (number/mm^2)	Volume fraction (%)	Surface area (mm^2/mm^3)	Diameter (μm)
True capillaries						
Median eminence zones						
Subependymal	0.44	96	221±31	1.0±0.1	5.4±0.5	5.0±0.2
Internal	1.01	162	147±31	0.5±0.1	3.2±0.8	4.5±0.2
External	0.97	626	655±87[a]	3.2±0.4[a]	17.1±2.0[a]	5.3±0.2[b]
Arcuate nucleus zones						
Proximal	0.58	125	234±78	0.9±0.2	5.1±1.5	5.0±0.2
Distal	3.23	585	171±21	0.6±0.1	3.6±0.4	4.7±0.1
Critical difference			*173*	*0.8*	*4.1*	*0.7*
Sinusoidal capillaries						
Median eminence zones						
Subependymal	0.44	49	105±27	1.7±0.4	5.4±1.3	10.8±0.4
Internal	1.01	42	37±11	0.6±0.2	1.9±0.6	11.4±0.8
External	0.97	374	424±45[a]	10.0±1.4[a]	25.8±2.8[a]	12.3±0.8
Arcuate nucleus						
Proximal	0.58	37	63±17	1.4±0.5	3.7±1.0	11.6±2.1
Critical difference			*130*	*3.3*	*7.4*	*ns*

Values are means±SE for 5 rats. *Critical difference* is the minimum value needed for significance between any two means. (ANOVA; $P<0.05$). ns, Not significant ($P>0.05$)

[a] External zone significantly greater than all other median eminence and arcuate nucleus zones

[b] External zone significantly greater than internal zone ($P<0.05$)

The arcuate nucleus was analyzed in two subregions (Fig. 1). A proximal zone was defined as the portion of the arcuate nucleus bordering the median eminence medially where tuberal perikarya were evident (Fig. 1). It contained a sparse number of Type-III sinusoidal vessels closely bordering the median eminence, but mostly had capillaries of Type-I and -II structure (Fig. 2D, E); it measured approximately 100 μm in the mediolateral width, with an average area bilaterally of 0.03 mm^2 in each section studied. A distal zone, defined as the remainder of the arcuate nucleus at the infundibular and lateral margins of the third ventricle medially and ventromedial nucleus dorsolaterally, measured approximately 0.16 mm^2 in total bilateral area per section. Only Type-II capillaries were found in this part of the arcuate nucleus.

Capillary dimensions across zones of the median eminence and arcuate nucleus. We analyzed a total of 884 true capillaries in the median eminence and 710 in two zones of the arcuate nucleus (Table 2). We also obtained data from 465 sinusoidal capillaries in the median eminence and 37 sinusoidal microvessels in the proximal arcuate nucleus (Table 2).

The density, volume fraction, and surface area of true and sinusoidal capillaries were largest in the external zone of the median eminence (Table 2). A combination of densities for both capillary types (true = 655/mm^2; sinusoids = 424/mm^2) gave a total value of 1079/mm^2 for the external zone of the median eminence. In contrast, in the adjacent palisade and internal zone of the median eminence, the total capillary density was 184/mm^2 (values in Table 2). Similar comparisons could be made for capillary volume and surface area in the external zone where values greatly exceeded those for dorsal parts of the median eminence and proximal arcuate nucleus (Table 2).

Capillary diameter in the external zone (5.3 μm) was larger than that of all other zones studied but this difference was significant ($P<0.05$) relative only to the internal zone (4.5 μm, Table 2). However, there was a tendency for all capillary dimensions in the subependymal zone of the median eminence, and the proximal zone of arcuate nucleus, to be larger than those in the internal zone of the median eminence and distal arcuate nucleus (for which measurements were similar, Table 2).

Sinusoid density, volume fraction, and surface area in the median eminence external zone significantly exceeded the dimensions of those of other median eminence zones and the proximal arcuate nucleus (Table 2). These measurements also tended to be larger in the ependymal and subependymal zone compared with the internal median eminence and proximal arcuate nucleus ($P>0.05$). Sinusoid diameter, averaging 11.5 μm, did not differ significantly across zones (Table 2). Sinusoidal capillaries were not present in the distal zone of the arcuate nucleus.

Pericapillary spaces. Pericapillary spaces around Type-I and -III capillaries were evident within all zones of the median eminence and around Type-I capillaries in the proximal arcuate nucleus, but not around Type-II capillaries of the distal arcuate nucleus (Fig. 2). The pericapillary space fraction, expressed as the percentage of tissue area occupied by the space between capillary basal la-

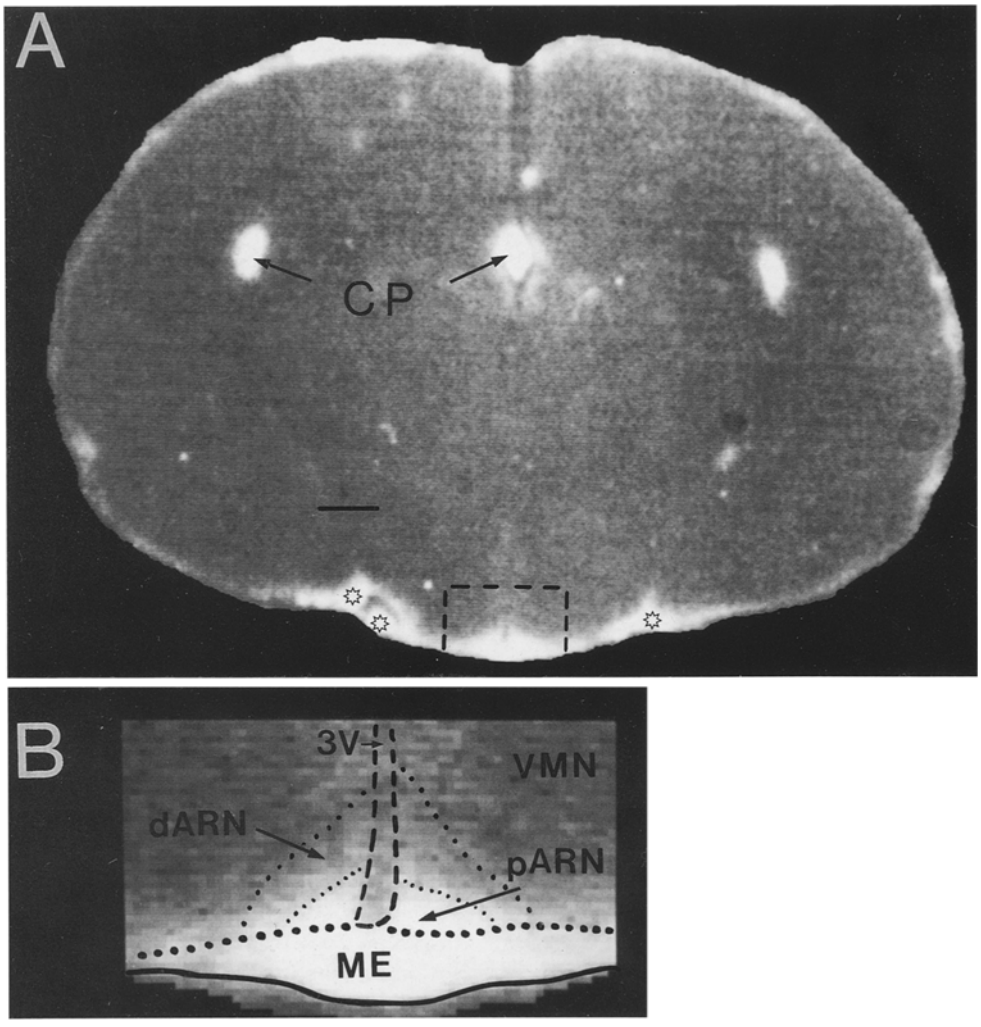

Fig. 3A, B. [^{14}C]AIB autoradiograph of the median eminence-arcuate nucleus region showing the subregional distribution of tracer circulated for 12 s. *Box* in **A** is redisplayed as **B**. *Bar* in **A** 1 mm; magnification of **B** = 4×. The boundaries of the subregions shown were approximated from the examination of magnified histological sections. The whiteness in the images is proportional to the relative density of the tracer deposition. *CP* Lateral and third ventricular choroid plexus; *3V* third ventricle; *VMN* ventromedial nucleus; *dARN* distal arcuate nucleus; *pARN* proximal arcuate nucleus; *ME* median eminence; *stars* in A, meninges and superior hypophysial arteries (see Ambach et al. 1976; Page et al. 1978)

minae, was much greater for Type-III capillaries in the external zone of the median eminence (14 ± 1.4%, $P < 0.05$) than in the internal and subependymal zones, which did not differ significantly (1 ± 0.3% and 3 ± 1.3%, respectively, $P > 0.05$). The pericapillary space fraction of Type-I capillaries in the proximal arcuate nucleus measured 1 ± 0.3%.

Electron microscopy

Type-III capillaries, characterized by numerous fenestrations, cytoplasmic vesicles or pits, and wide pericapillary labyrinths between the parenchymal and capillary basal laminae (Table 1, Fig. 2A), were the only type found in the median eminence external zone. In many of the Type-III capillaries, we identified fenestral discontinuities, or pores, in the endothelial membrane bilayer (Fig. 2A). Type-III capillaries were also present, although were far less numerous than in the portal plexus, or in the internal and subependymal zones of the median eminence. We could not discern whether these vessels were the dorsal segments of the primary plexus loops described previously (e.g., Duvernoy 1972; Ambach et al. 1976; Page et al. 1978). All sinusoidal capillaries (i.e., with diameters > 7.5 μm) had Type-III endothelium. No true capillaries in the proximal arcuate nucleus were of the Type-III morphology, but we did identify a sparse number of Type-III sinusoids in the transitional zone between the median eminence and arcuate nucleus (Table 2).

In the internal and subependymal zones of the median eminence, and in the proximal arcuate nucleus, we found a high incidence of Type-I capillaries, notable for their lack of fenestrations, moderate vesicular density, and narrow, but measurable, pericapillary spaces (Table 1, Fig. 2B–D).

Type-II capillaries, typical of those forming the BBB in most of the nervous system (Marchesi and Barrnett 1964; Shaver et al. 1990), were present in the proximal arcuate nucleus and were the only type observed in the distal arcuate and ventromedial nuclei (Fig. 2E; Gross et al. 1986).

Microvascular physiology. The pre-experiment assessment of various measurements reflecting the physiological status of the 17 conscious rats provided the following profile; all data were obtained within 5 min of starting the tracer studies. Mean body weight for the group (± SE) was 398 ± 18 g. Body temperature was

Table 3. Microvascular volume, blood flow, and capillary permeability in subregions of the basal hypothalamus in rats. Experiments to determine AIB blood-tissue transfer, extraction, and *PS* products were 12 s in duration. AIB, [^{14}C]α-aminoisobutyric acid; PS, permeability × surface area product

Structures (*n*)	Exchangeable volume (μl g^{-1}) (6)	Capillary blood flow (μl g^{-1} min^{-1}) (5)	Capillary plasma flow (μl g^{-1} min^{-1})	AIB transfer constant (μl g^{-1} min^{-1}) (6)	Sucrose transit time (s)	AIB extraction (%)	AIB *PS* product (μl g^{-1} min^{-1})
Median eminence	39±4[a]	2433±309[a]	1752	266±67[a]	1.3	15	285
Arcuate nucleus zones							
Proximal	16±2[a]	1333±88	906	69±23[a]	1.1	8	69
Distal	4±1	1140±21	775	2±2	0.3	<1	2
Ventromedial nucleus	4±1	928±54	631	2±1	0.4	<1	2

Values are means±SE for the number of rats in parentheses. See Equations 1–7 for derivations

[a] Significantly different from values for distal arcuate or ventromedial nuclei (*F* test with $P<0.05$)

37.0±0.10° C and mean arterial pressure and hematocrit were 115±2 mm Hg and 46±1%, respectively. Arterial blood gases and pH: PO_2 equaled 87±2 mm Hg; PCO_2 was 39±1 mm Hg; pH was 7.43±0.01. The arterial plasma value for glucose was 1.75±0.20 mg/ml; for Na^+, 143.4±0.54 mmol/l; for K^+, 4.50±0.05 mmol/l; for Ca^{2+}, 1.38±0.01 mmol/l. All these measurements fall within the range of normal values for conscious, unstressed rats (e.g., Gross et al. 1987, 1990).

Our autoradiographic and image analysis of microvascular physiological properties in the median eminence and basal hypothalamus was limited to comparisons between the whole median eminence, a zone of the arcuate nucleus proximal to the median eminence (width of 75–125 μm), one zone of the arcuate nucleus distal from the median eminence, and the ventromedial nucleus (Fig. 3A, B).

Exchangeable volume (30-s[^{14}C]sucrose space), a measure indicative of microvascular richness (Gross et al. 1987, 1990), was more than twice as large in the median eminence as in the proximal arcuate nucleus, and 10× greater than in the distal arcuate or ventromedial nuclei (Table 3).

Rates of capillary blood and plasma flow in the median eminence were significantly greater than those in the distal arcuate or ventromedial nuclei by about 2×; comparisons of blood flow among other regions did not reveal significant differences (Table 3). Considerably higher values for unidirectional influx, extraction, and *PS* product for single circulations of the permeability marker, [^{14}C]AIB, were found in the median eminence compared with other zones (Table 3; Fig. 3A, B). An intriguing finding, however, was that AIB transfer, extraction, and *PS* were substantially greater in the proximal arcuate than in the distal arcuate nucleus (*PS* products for [^{14}C]AIB of 69 vs. 2 μl g^{-1} min^{-1}, Table 3, Fig. 3B).

Calculation of the duration of transit of the plasma marker, [^{14}C]sucrose, through individual microcirculations revealed a slower circulation through the median eminence and proximal arcuate nucleus (1.1 to 1.3 sec) compared with that in the distal arcuate or ventromedial nuclei (about 0.4 s, Table 3).

Discussion

There were three important morphological findings of the present study. Firstly, three distinct types of capillary, classified by ultrastructural criteria, were identified in the median eminence-arcuate nucleus complex. The capillary distribution according to these ultrastructural criteria bore the following general topography: Type-III capillaries were present throughout the median eminence but lay primarily in the external zone; Type-I capillaries were found in the internal and subependymal zones of the median eminence, and in the proximal subdivision of the arcuate nucleus; Type-II capillaries occurred in both the proximal and distal subdivisions of the arcuate nucleus. Secondly, the density and surface area of Type-III capillaries in the median eminence external zone were quantified by morphometric imaging methods and found to be 3–5 times larger than those of capillary networks in other zones of the median eminence or tuberal hypothalamus. Capillary densities in the arcuate nucleus did not differ significantly from those in subependymal and internal zones of the median eminence. Finally, a distinguishing feature of the capillary network in the proximal arcuate nucleus was the presence around Type-I capillaries of measurable Virchow-Robin spaces (1% of tissue area). Although this finding is not new (see Krisch et al. 1978), our results demonstrate that the volume of arcuate pericapillary spaces is quantitatively similar to that in the dorsocentral median eminence. These results collectively suggest that a common, extravascular pathway exists via which arcuate neurons can be modified humorally by median eminence factors.

Our physiological studies have provided three new sets of quantitative results: (1) microvascular exchangeable volume, i.e., the volume of the capillary and perivascular space available for blood-tissue solute exchange, was 4–10 times larger in the proximal arcuate nucleus and median eminence than in the distal arcuate or ventromedial nuclei; (2) the capillary *PS* product for [^{14}C]AIB, an index of the rate of tissue penetration by blood-borne physiological substances, was 34–142 times greater in the proximal arcuate nucleus and median emi-

nence than in the distal arcuate or ventromedial nuclei; and (3) the duration of transit for tracer sucrose (and probably for circulating hormones or other neuroactive substances) through the microvascular networks of the proximal arcuate nucleus and median eminence was about 3 times longer than that through microcirculations in the distal arcuate or ventromedial nuclei.

Thus, the quantitative experiments revealed some unusual morphometric and physiological characteristics for specialized, differentiated microvascular beds of the tuberoinfundibular system. We shall discuss the results in the context of their relationship to the cytoarchitectural and chemical topography of these tuber cinereum structures, the significance of physiological dissimilarities in microvascular properties, and the apparent role of confluent Virchow-Robin spaces in contributing to neurohumoral functions of the arcuate nuclei.

Topographical relationship of capillary dimensions to tuberoinfundibular cytoarchitecture and cytochemistry

We subdivided the tuberoinfundibular system into 5 zones for the morphometric analysis, viz., 3 in the median eminence and 2 in the arcuate nucleus. The external, internal, and subependymal layers of the median eminence were identified on the basis of angio- and cytoarchitecture described previously (Duvernoy and Koritké 1964; Duvernoy 1972; Monroe et al. 1972; Weindl and Joynt 1972; Ambach et al. 1976). The external zone, characterized by the primary portal plexus amid wide pericapillary labyrinths (Fig. 1), had a measured density of 1079 true and sinusoidal capillaries/mm^2, a number exceeding that of any other subdivision of the tuberal hypothalamus by 3–5 times. Capillary densities in the internal and subependymal zones of the median eminence, and in two subregions of the arcuate nucleus, did not differ significantly. Cytologically, however, these tissue regions vary considerably, since the internal zone is a tract of axonal and tanycytic trunks, the subependymal zone is a network of β_1- and β_2-tanycytic perikarya rich in innervation by peptidergic neurons, and the arcuate nucleus is the source of a diversity of POMC- and other peptidergic or aminergic perikarya and neuropil (Monroe et al. 1972; Akmayev and Fidelina 1976; Rodríguez et al. 1979; Palkovits 1982; Mezey et al. 1985; Kiss et al. 1985; Mezey 1987). Thus, although the differentiation of capillary networks among zones in the median eminence has been recognized subjectively for many years (e.g., Duvernoy and Koritké 1964; Duvernoy 1972; Ambach et al. 1976; Page et al. 1978), the present studies furnish quantitative evidence for the magnitude of capillary bed differentiation in median eminence layers, and reveal that dorsal zones of the median eminence do not differ substantially in capillarity compared with the adjacent hypothalamic arcuate nuclei, despite marked differences in cytology and function.

An interesting finding discussed previously by others (Hisano et al. 1982; Mezey and Palkovits 1982; Kiss et al. 1985) and confirmed here is that capillary density is low in the subependymal and internal zones where major neurochemical projections to the median eminence terminate (e.g., see Kiss et al. 1985; Mezey 1987) (Fig. 1, Table 2). Some of these fibers may innervate β_2-tanycytes making specialized contacts with Type-I capillaries (Rodríguez et al. 1979), and thus could provide neurohumoral control over these vessels.

Immunoreactivity for numerous peptides and amines shows a specific topographical distribution in the subependymal and internal zones of the median eminence; included among these are somatostatin, neurophysin, oxytocin, corticotropin-releasing hormone, galanin, cholecystokinin, prolactin, neuropeptide Y, opioid peptides, and norepinephrine (Weindl and Sofroniew 1978; Moore and Bloom 1979; Mezey 1987). Hisano et al. (1982) reported that some POMC terminals invaded pericapillary spaces of the subependymal zone. Since Virchow-Robin spaces in the subependymal and internal zones are thought to be confluent with those around external zone portal capillaries, and with spaces around capillaries in the arcuate nucleus (Török 1964; Mezey and Palkovits 1982), secretions of POMC or other peptides into pericapillary spaces in the median eminence may reach all parts of the tuber cinereum (see further discussion below). External zone capillaries are the destination of numerous other peptidergic and aminergic systems projecting to the median eminence from the hypothalamus and brainstem (Palkovits 1982; Mezey 1987). Additionally, the distribution of immunoreactivity for peptidergic neurons in the arcuate nucleus (e.g., Mezey et al. 1985; Mezey 1987) coincides topographically with the extent of tissue labeling by blood-borne markers, such as [^{14}C]AIB in the present study (Fig. 3B). Thus, there may be considerable feedback via humoral pathways to arcuate neurons by the same substances secreted from peptide-producing cells and their processes in all zones of the median eminence (Mezey and Palkovits 1982; van den Pol and Cassidy 1982).

In the external zone of the median eminence, the diameter of Type-III true capillaries was found to be wider (5.3 μm vs. 5.0 μm or less elsewhere, Table 2), and the density of sinusoids was greater than elsewhere in the median eminence. We were not able to measure intravascular pressures or the rate of blood flow subregionally in the median eminence (Table 3), but if we assume uniformity of these physiological properties for individual capillary beds across the zones of the median eminence, a wider diameter indicates that intracapillary hydrostatic pressure, linear blood velocity, and resistance to blood flow must be lower in the external zone. Consequently, subregional differences in solute filtration across capillary endothelial cells can be expected in the median eminence.

The morphometric analysis of capillary networks in the tuber cinereum permits comparisons with results for other circumventricular organs and gray matter. The median eminence external zone has a vascularization similar in density to that of the pituitary neural lobe and hypothalamic magnocellular nuclei, viz., values of about 1000 capillaries/mm^2, which are the highest determined to date for structures in the nervous system (Craigie 1940; Sposito and Gross 1987a; Gross 1991). Circum-

ventricular organs, including the subfornical organ and area postrema, have capillary densities of about 500/mm^2 (Sposito and Gross 1987b; Shaver et al. 1991). Dorsocentral zones of the median eminence and arcuate nuclei, however, have a low capillarity, like that of the hypothalamic ventromedial nuclei (about 200/mm^2; Gross et al. 1986), thought by Craigie (1940) to be among the lowest capillary densities for any cerebral gray matter structures.

Dissimilarities in microvascular physiological properties of tuberoinfundibular subregions

[^{14}C]AIB has been used effectively as a tracer for quantitative autoradiographic analysis of BBB properties (Blasberg et al. 1983a, b) and for its rates of penetration across permeable circumventricular organ capillaries (Gross et al. 1986, 1987, 1990). Because of its advantageous characteristic of avid uptake by neurons and glial cells (Blasberg et al. 1983a), unidirectional transfer can be assumed reasonably to mimic the fate of brain-bound hormones interacting with tuberal endothelial and parenchymal cells.

The most striking quantitative result of the physiological studies was the magnitude of PS product for [^{14}C]AIB in the proximal arcuate nucleus (69 μl g^{-1} min^{-1}) compared with its distal segment bordering the ventromedial nucleus (2 μl g^{-1} min^{-1}). Over the mediolateral breadth of this small tissue zone, a distance of some 150 μm or less from the lateral border with median eminence (Fig. 3B), the influx of tracer was 35 times greater than in the adjacent, more distal zone of the same nucleus during a single circulation lasting less than 12 s. Although observed previously for larger blood tracers and circulation times of several minutes or longer (Wsniewski and Olszewski 1963; Brightman et al. 1975; Broadwell and Brightman 1976; van den Pol and Cassidy 1982; Balin et al. 1986; Martinez and Koda 1988), this result was surprising since the proximal arcuate nucleus has mostly Type-II impermeable capillaries that are low in total density (Table 2).

Labeling of arcuate parenchyma by retrograde axonal transport of substances, such as HRP, from the median eminence has previously been demonstrated (Broadwell and Brightman 1976). However, the ultrastructure of the arcuate capillary bed includes Type-I true capillaries and Type-III sinusoids in the proximal zone (Fig. 2D), vessels considered highly permeable to macromolecules (Marchesi and Barrnett 1964; Rhodin 1974; Shaver et al. 1990). These capillaries may be significant sites of leakage by circulating substances into the tuber. It is possible that [^{14}C]AIB infiltrated arcuate regions via transcapillary routes, or it may have followed the paravascular pathways discussed below. Whatever the mechanism of tracer influx to the proximal arcuate nucleus, the results indicate that blood-borne hormones from the systemic circulation via the median eminence, or via pericapillary spaces, could gain rapid access to this tuberal subregion. The spread of humoral substances further laterally toward the ventromedial nucleus appears to be well-demarcated within the medial arcuate nucleus, probably because of tight pericapillary sheathing by β_1- and α_2-tanycytic processes (Krisch et al. 1978; Rodríguez et al. 1979; van den Pol and Cassidy 1982; Réthelyi 1984).

PS products for the median eminence and distal arcuate nucleus demonstrated a marked contrast in capillary permeability between these parts of the tuber cinereum. The *PS* product of 285 μl g^{-1} min^{-1} measured in this study for the median eminence, similar to the 12-s influx rates for [^{14}C]AIB in other circumventricular organs (Gross et al. 1987, 1990), was 142 times larger than in BBB territories of the distal tuber. These results provide reasonable approximations for the rate of permeation and tissue distribution of hormones in tuber cinereum subregions during a single circulation of hormone molecules through the respective capillary networks.

A physiological index of vascularization, the 30-s exchangeable volume measurement using [^{14}C]sucrose (Ohno et al. 1978; Gross et al. 1990), showed that the microvascular space available for blood-tissue exchange in the proximal arcuate nucleus was, unexpectedly, 4-fold larger than in the neighboring distal arcuate and ventromedial nuclei (16 vs 4 μl g^{-1}, Table 3). In capillary networks like those of the tuberoinfundibular system, the sucrose space cannot be judged as strictly intravascular, but probably includes perivascular spaces marked by extravasated tracer (Gross et al. 1987). For example, in the same way as the *PS* products differed between the median eminence and distal arcuate nucleus (Table 3), the exchangeable volume varied from 39 μl g^{-1} in the vascular-rich median eminence to 4 μl g^{-1} in the distal arcuate and ventromedial nuclei, both of which have a low capillary density (Table 2). The magnitude of difference between the median eminence and distal tuber for the exchangeable volume determinations (about 10:1, Table 3), however, was larger than that for the actual capillary density (about 5:1 using the median eminence external zone values, Table 2), an outcome probably resulting from extravasated tracer in the median eminence. The exchangeable space measurement is nonetheless meaningful because it labels compartments into which blood-borne hormones (having a similar hydrodynamic radius, molecular weight, and solubility as sucrose) would permeate over equivalent circulation periods. Furthermore, the term of exchangeable volume, used in the solution of unidirectional transfer and the *PS* product of [^{14}C]AIB (Eq. 3–6), represents the space of the entire exchange surface between blood and brain, including the endothelium and perivascular spaces (Renkin 1959; Gross et al. 1990).

Calculation of the transit time of [^{14}C]sucrose through these tuberoinfundibular microcirculations indicated a difference of about 3-fold between the briskly perfused distal arcuate and ventromedial nuclei (transit times of about 0.4 s) and the more protracted irrigation of the median eminence and proximal arcuate nucleus (transit times of about 1.2 s). This finding is similar to that obtained for other circumventricular organs (Gross et al. 1987, 1990; Gross 1991), and so may represent a common characteristic of neuroendocrine microcircula-

tions; in the proximal arcuate nucleus, median eminence, and other circumventricular organs, blood-borne solutes have prolonged circulation times that probably facilitate parenchymal sensory or secretory properties.

Dispersive role of Virchow-Robin spaces in tuberoinfundibular subregions

An interesting result of the present experiments was the labeling of the proximal arcuate nucleus by blood-derived [^{14}C]AIB within a few seconds of intravenous administration (Fig. 3 B). Since arcuate capillaries are mostly of the Type-II ultrastructure, and are thus presumed to be impermeable, the results indicate that AIB must have penetrated rapidly and extensively across the small number of Type-I and Type-III capillaries, or was transported into the hypothalamus via paravascular routes suspected previously of contributing median eminence factors to the tuber (Leonhardt and Eberhardt 1972; Mezey and Palkovits 1982). Substances in median eminence blood or pericapillary spaces, deriving from the systemic or pituitary circulation, or from tuberoinfundibular axon terminals, would have access to the proximal arcuate nucleus via communicating pericapillary channels (Krisch et al. 1978; Mezey and Palkovits 1982).

A previous analysis of such a route within the brain by Rennels and coworkers (1985) suggested that material suspended in the cerebrospinal fluid of pericapillary spaces could be agitated and propagated along the microvascular network by pulsations of nearby resistance vessels, thus creating paravascular pressure gradients with the heart beat. In our experiments, we can assume that approximately half of the time (about 6 s) following [^{14}C]AIB injection was required to transport the tracer from the blood through the interstitial spaces in the arcuate nucleus. Thus, tracer dispersal would have occurred over some 35 heart beats in the conscious rat (heat rate of 350 beats/min) in 0.1 min. Favorable microvascular design for such pericapillary dispersion exists in the median eminence where superior hypophysial arterioles penetrate as a ring around the borders of, and throughout, the portal capillary plexus, much of which lies within expansive Virchow-Robin labyrinths, and which is continuous with capillaries in other median eminence zones and the arcuate nucleus (Wislocki and King 1936; Török 1964; Ambach et al. 1976; Page et al. 1978).

Wsniewski and Olszewski (1963), studying the tissue distribution of radiolabeled albumin or gamma globulin in the median eminence-arcuate nucleus complex of cats, reported the same type of tracer dispersal as observed in our experiments. An important insight from their analysis was the finding that no radioactivity labeled the arcuate nuclei when the tracer was perfused postmortem (their Fig. 10), a condition that would of course lack the propulsive influence of heart beats.

In conclusion, part of the titer of neurohumoral substances at the interface of the median eminence and its capillary blood may be propelled centrifugally by arteriolar pressure pulses via confluent Virchow-Robin spaces over a period of just a few seconds. If such a mechanism exists in vivo, then proximal arcuate neurons would be under interstitial irrigation by a neurohumoral admixture streaming perpetually from the median eminence.

Acknowledgements. We thank Jennifer Hamilton for assistance with the preparation of the manuscript. The studies were supported by grants from the Medical Research Council of Canada, the Heart and Stroke Foundation of Ontario, and the Ontario Ministry of Colleges and Universities. K.M.W. is a Research Fellow with the Medical Research Council. P.M.G. is a Research Scholar with the Heart and Stroke Foundation of Ontario.

References

Akmayev IG, Fidelina OV (1976) Morphological aspects of the hypothalamic-hypophyseal system VI. The tanycytes: their relation to the sexual differentiation of the hypothalamus. An enzyme-histochemical study. Cell Tissue Res 173:407–416

Ambach G, Palkovits M, Szentágothai J (1976) Blood supply of the rat hypothalamus. IV. Retrochiasmatic area, median eminence, arcuate nucleus. Acta Morphol Acad Sci Hung 24:93–119

Balin BJ, Broadwell RD, Salcman M, El-Kalliny M (1986) Avenues for entry of peripherally administered protein to the central nervous system in mouse, rat, and squirrel monkey. J Comp Neurol 251:260–280

Blasberg RG, Fenstermacher JD, Patlak CS (1983a) Transport of α-aminoisobutyric acid across brain capillary and cellular membranes. J Cereb Blood Flow Metab 3:8–32

Blasberg RG, Patlak CS, Fenstermacher JD (1983b) Selection of experimental conditions for the accurate determination of blood-brain transfer constants from single-time experiments: a theoretical analysis. J Cereb Blood Flow Metab 3:215–225

Brightman MW, Prescott S, Reese TS (1975) Intercellular junctions of special ependyma. In: Knigge KM, Scott DE, Kobayashi H, Ishii S (eds) Brain-endocrine interaction II. The ventricular system in neuroendocrine mechanisms. Karger, Basel, pp 146–165

Broadwell RD, Brightman MW (1976) Entry of peroxidase into neurons of the central and peripheral nervous systems from extracerebral and cerebral blood. J Comp Neurol 166:257–284

Broadwell RD, Brightman MW (1983) Horseradish peroxidase: a tool for study of the neuroendocrine cell and other peptide-secreting cells. Methods Enzymol 103:187–218

Craigie EH (1940) Measurements of vascularity in some hypothalamic nuclei of the albino rat. Res Publ Assoc Res Nerv Ment Dis 20:310–319

Crone C (1963) The permeability of capillaries in various organs as determined by the use of the 'indicator diffusion' method. Acta Physiol Scand 58:292–303

Duvernoy H (1972) The vascular architecture of the median eminence. In: Knigge KM, Scott DE, Weindl A (eds) Brain-endocrine interaction. Median eminence: structure and function. Karger, Basel, pp 79–108

Duvernoy H, Koritké JG (1964) Contribution à l'étude de l'angioarchitectonie des organes circumventriculaires. Arch Biol [Suppl] (Liège) 75:849–904

Gross PM (1991) Morphology and physiology of capillary systems in subregions of the subfornical organ and area postrema. Can J Physiol Pharmacol 69:1010–1025

Gross PM, Sposito NM, Pettersen SE, Fenstermacher JD (1986) Differences in function and structure of the capillary endothelium in the supraoptic nucleus and pituitary neural lobe of rats. Neuroendocrinology 44:401–407

Gross PM, Blasberg RG, Fenstermacher JD, Patlak CS (1987) The microcirculation of rat circumventricular organs and pituitary gland. Brain Res Bull 18:73–85

Gross PM, Wall KM, Pang JJ, Shaver SW, Wainman DS (1990) Microvascular specializations promoting rapid interstitial solute dispersion in nucleus tractus solitarius. Am J Physiol 259:R1131–R1138

Hisano S, Kawano H, Nishiyama T, Daikoku S (1982) Immunoreactive ACTH/β-endorphin neurons in the tubero-infundibular hypothalamus of rats. Cell Tissue Res 224:303–314

Hökfelt T, Fuxe K (1972) On the morphology and the neuroendocrine role of the hypothalamic catecholamine neurons. In: Knigge KM, Scott DE, Weindl A (eds) Brain-endocrine interaction. Median eminence: structure and function. Karger, Basel, pp 181–223

Kiss JZ, Mezey E, Cassell MD, Williams TH, Mueller GP, O'Donohue TL, Palkovits M (1985) Topographical distribution of pro-opiomelanocortin-derived peptides (ACTH/β-END/α-MSH) in the rat median eminence. Brain Res 329:169–176

Krisch B, Leonhardt H (1989) Relations between leptomeningeal compartments and the neurohemal regions of circumventricular organs. Biomed Res 10:155–168

Krisch B, Leonhardt H, Buchheim W (1978) The functional and structural border of the neurohemal region of the median eminence. Cell Tissue Res 192:327–339

Leonhardt H, Eberhardt HG (1972) Dye transport from the median eminence to the hypothalamic wall. In: Knigge KM, Scott DE, Weindl A (eds) Brain-endocrine interaction. Median eminence: structure and function. Karger, Basel, pp 335–341

Marchesi VT, Barrnett RJ (1964) The localization of nucleoside-phosphatase activity in different types of small blood vessels. J Ultrastruct Res 10:103–115

Martinez JL, Koda L (1988) Penetration of fluorescein into the brain: a sex difference. Brain Res 450:81–85

Mezey E (1987) The median eminence and pituitary gland: chemistry of neural inputs. In: Gross PM (ed) Circumventricular organs and body fluids, vol II. CRC Press, Boca Raton, pp 87–108

Mezey E, Palkovits M (1982) Two-way transport in the hypothalamo-hypophyseal system. In: Ganong WF, Martini L (eds) Frontiers in neuroendocrinology, vol 7. Raven Press, New York, pp 1–29

Mezey E, Kiss JZ, Mueller GP, Eskay R, O'Donohue TL, Palkovits M (1985) Distribution of the pro-opiomelanocortin derived peptides, adrenocorticotrope hormone, α-melanocyte-stimulating hormone and β-endorphin (ACTH, α-MSH, β-END) in the rat hypothalamus. Brain Res 328:341–347

Monroe BG, Newman BL, Schapiro S (1972) Ultrastructure of the median eminence of neonatal and adult rats. In: Knigge KM, Scott DE, Weindl A (eds) Brain-endocrine interaction. Median eminence: structure and function. Karger, Basel, pp 7–26

Moore RY, Bloom FE (1979) Central catecholamine neuron systems: anatomy and physiology of the norepinephrine and epinephrine systems. Annu Rev Neurosci 2:113–168

Ohno K, Pettigrew KD, Rapoport SI (1978) Lower limits of cerebrovascular permeability to nonelectrolytes in the conscious rat. Am J Physiol 235:H299–H307

Page RB (1982) Pituitary blood flow. Am J Physiol 243:E427–E442

Page RB, Leure-Dupree AE, Bergland RM (1978) The neurohypophyseal capillary bed. II. Specializations within median eminence. Am J Anat 153:33–65

Palkovits M (1982) Neuropeptides in the median eminence: their sources and destinations. Peptides 3:299–303

Paxinos G, Watson C (1986) The rat brain in stereotaxic coordinates, 2nd edn. Academic Press, New York

Pol AN van den, Cassidy JR (1982) The hypothalamic arcuate nucleus of the rat – a quantitative Golgi analysis. J Comp Neurol 204:65–98

Renkin EM (1959) Transport of potassium-42 from blood to tissue in isolated mammalian skeletal muscles. Am J Physiol 197:1205–1210

Rennels ML, Gregory TF, Blaumanis OR, Fujimoto K, Grady PA (1985) Evidence for a 'paravascular' fluid circulation in the mammalian central nervous system, provided by the rapid distribution of tracer protein throughout the brain from the subarachnoid space. Brain Res 326:47–63

Réthelyi M (1984) Diffusional barrier around the hypothalamic arcuate nucleus in the rat. Brain Res 307:355–358

Rhodin JAG (1974) Histology: a text and atlas. Oxford University Press, New York, pp 352–358

Rodríguez EM (1972) Comparative and functional morphology of the median eminence. In: Knigge KM, Scott DE, Weindl A (eds) Brain-endocrine interaction. Median eminence: structure and function. Karger, Basel, pp 319–334

Rodríguez EM (1976) The cerebrospinal fluid as a pathway in neuroendocrine integration. J Endocrinol 71:407–443

Rodríguez EM, González CB, Delannoy L (1979) Cellular organization of the lateral and postinfundibular regions of the median eminence in the rat. Cell Tissue Res 201:377–408

Sakurada O, Kennedy C, Jehle J, Brown JD, Carbin G, Sokoloff L (1978) Measurement of local cerebral blood flow with iodo[^{14}C]antipyrine. Am J Physiol 234:H59–H66

Shaver SW, Sposito NM, Gross PM (1990) Quantitative fine structure of capillaries in subregions of the rat subfornical organ. J Comp Neurol 294:145–152

Shaver SW, Pang JJ, Sposito NM, Wall KM, Gross PM (1991) Subregional topography of capillaries in the dorsal vagal complex of rats. I. Morphometric properties. J Comp Neurol 306:73–82

Sposito NM, Gross PM (1987a) Morphometry of individual capillary beds in the hypothalamo-neurohypophysial system of rats. Brain Res 403:375–379

Sposito NM, Gross PM (1987b) Topography and morphometry of capillaries in the rat subfornical organ. J Comp Neurol 260:36–46

Szentágothai J, Flerkó B, Mess B, Halász B (1968) Hypothalamic control of the anterior pituitary. An experimental-morphological study. Akadémiai Kiadó, Budapest, pp 81–109

Török B (1964) Structure of the vascular connections of the hypothalamo-hypophysial region. Acta Anat 59:84–99

Weibel EW, Kistler GS, Scherle WF (1966) Practical stereological methods for morphometric cytology. J Cell Biol 30:23–38

Weindl A, Joynt RJ (1972) The median eminence as a circumventricular organ. In: Knigge KM, Scott DE, Weindl A (eds) Brain-endocrine interaction. Median eminence: structure and function. Karger, Basel, pp 280–297

Weindl A, Sofroniew MV (1978) Neurohormones and circumventricular organs. In: Scott DE, Kozlowski GP, Weindl A (eds) Brain-endocrine interaction III. Neural hormones and reproduction. Karger, Basel, pp 117–137

Wislocki GB, King LS (1936) The permeability of the hypophysis and hypothalamus to vital dyes with a study of the hypophyseal vascular supply. Am J Anat 58:421–472

Wsniewski H, Olszewski J (1963) Vascular permeability in the area postrema and hypothalamus: a study using iodinated radioactive albumin. Neurology 13:885–894